

Supporting Information

A highly stable MOF with F and N accessible sites for efficient capture and separation of acetylene from ternary mixture

Gang-Ding Wang,^a Hai-Hua Wang,^b Wen-Juan Shi,^a Lei Hou,^{*,a} Yao-Yu Wang^a and Zhonghua Zhu^c

^a*Key Laboratory of Synthetic and Natural Functional Molecule Chemistry of the Ministry of Education, National Demonstration Center for Experimental Chemistry Education (Northwest University), College of Chemistry & Materials Science, Northwest University. Xi'an, 710069, P. R. China.*

^b*College of Food Science and Engineering, Northwest A&F University. Yangling, Shaanxi 712100, China.*

^c*School of Chemical Engineering, The University of Queensland Brisbane 4072, Australia.*

*To whom correspondence should be addressed. E-mail: swjuan2000@126.com (Wen-Juan Shi), lhou2009@nwu.edu.cn (Lei Hou).

Molecular structure						
Molecular formula	Molecular dimension (Å)			Kinetic diameter (Å)	Polarizability $\times 10^{-25}$ (cm 3)	Boiling point (K)
	X	Y	Z			
C ₂ H ₂	3.32	3.34	5.70	3.33	33.3-39.3	188.4
C ₂ H ₄	3.28	4.18	4.84	4.16	42.5	169.4
C ₂ H ₆	3.81	4.08	4.82	4.44	44.3-44.7	184.6
CO ₂	3.2	3.3	5.4	3.33	29.11	194.7

Scheme S1. Structures and physical properties of C₂H₂, C₂H₄, C₂H₆ and CO₂.

X-ray crystallography

A Bruker Smart Apex II CCD detector was used to collect the single crystal data at 296(2) K using Mo K α radiation ($\lambda = 0.71073$ Å). The structure was solved by direct methods and refined by full-matrix least-squares refinement based on F2 with the SHELXTL program. The non-hydrogen atoms were refined anisotropically with the hydrogen atoms added at their geometrically ideal positions and refined isotropically. As the disordered solvent DMF molecules in the structure cannot be located, the SQUEEZE routine of Platon program was applied in refining. The formula of complex was got by the single crystal analysis together with elemental microanalyses and TGA data. Relevant crystallographic results are listed in Table S1. Selected bond lengths and angles are provided in Table S2.

N₂ sorption isotherm

Before gas sorption experiments, All the as-synthesized samples were immersed in CH₃OH for 72 hours, during which the solvent was decanted and freshly replenished four times a day. All the samples were activated under vacuum at 463 K for 6 hours. In addition, after removal of guest molecules leads to a color change from light blue to dark green for **1a** (Figure S7). Gas sorption measurements were then conducted using a Micrometrics ASAP 2020M gas adsorption analyzer.

Fitting adsorption heat of pure component isotherms

$$\ln P = \ln N + 1/T \sum_{i=0}^m a_i N^i + \sum_{i=0}^n b_i N^i \quad Q_{st} = -R \sum_{i=0}^m a_i N^i$$

The above virial expression was used to fit the combined isotherm data for **1a** at 273.15 and 298 K, where P is the pressure, N is the adsorbed amount, T is the temperature, ai and bi are virial coefficients, and m and N are the number of coefficients used to describe the isotherms. Q_{st} is the coverage-dependent enthalpy of adsorption and R is the universal gas constant.

Gas selectivity prediction via IAST

The experimental isotherm data for pure C₂, CH₄ were fitted using a dual Langmuir-Freundlich (L-F) model:

$$q = \frac{a_1 * b_1 * P^{c1}}{1 + b_1 * P^{c1}} + \frac{a_2 * b_2 * P^{c2}}{1 + b_2 * P^{c2}}$$

Where q and p are adsorbed amounts and the pressure of component i, respectively.

The adsorption selectivities for binary mixtures of C₂/CH₄, defined by

$$S_{i/j} = \frac{x_i * y_j}{x_j * y_i}$$

Were respectively calculated using the Ideal Adsorption Solution Theory (IAST). Where x_i is the mole fraction of component i in the adsorbed phase and y_i is the mole fraction of component i in the bulk.

Breakthrough experiments

The breakthrough experiment was performed on the Quantachrome dynaSorb BT equipments at 298 K and 1 bar with an equal volume of mixed gas (gas A: gas B: Ar = 5% : 5% : 90% or gas A: gas B: gas C: Ar = 5%: 5%: 5%: 85%, Ar as the carrier gas, flow rate = 8 mL/min). The activated **1a** (0.7 g) was filled into a packed column of ϕ 4.2×80 mm, and then the packed column was washed with Ar at a rate of 8 mL min⁻¹ at 70 °C for 60 minutes to further activate the samples. Between two breakthrough experiments, the adsorbent was regenerated by Ar flow of 8 mL min⁻¹ for 35 min at 80 °C to guarantee a complete removal of the adsorbed gases.

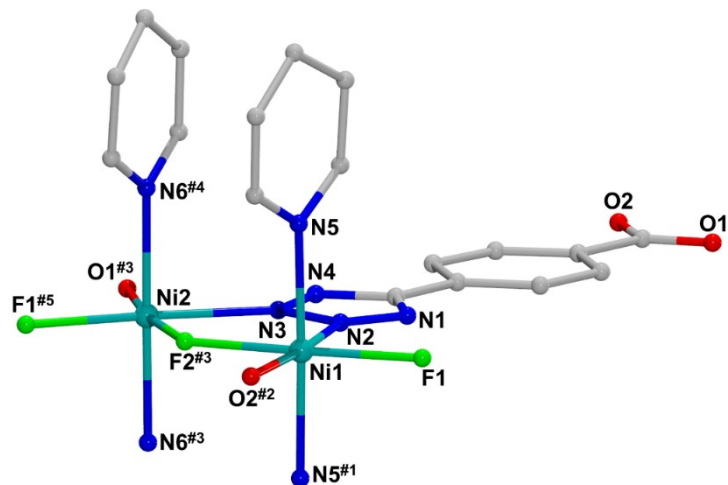


Fig. S1 Coordination environment of Ni^{2+} ion in **1**. Symmetry codes: #1 1-x, y, z; #2 x, -1+y, z; #3 1-x, 1-y, -0.5+z; #4 x, 1-y, -0.5+z; #5 1-x, -y, -0.5+z.

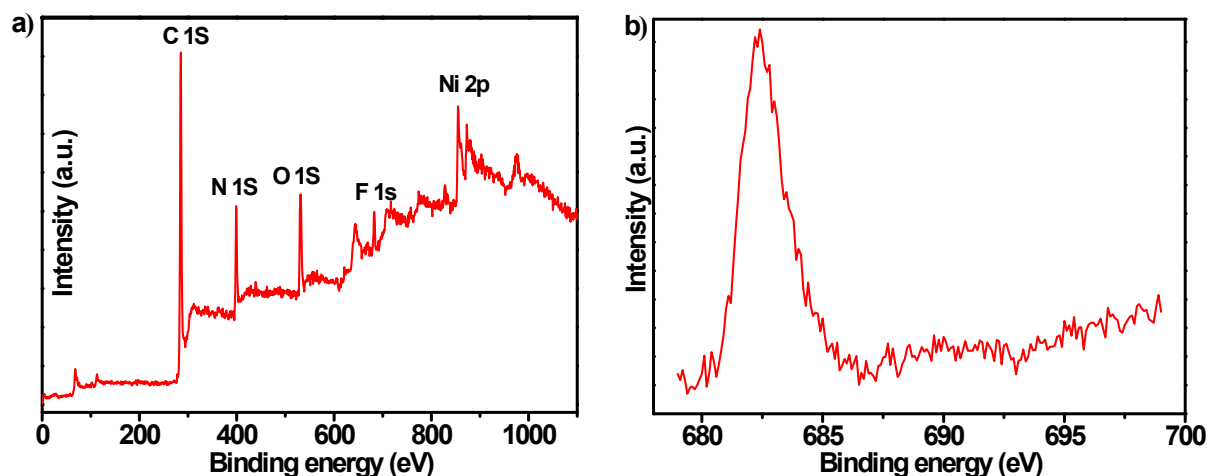


Fig. S2 XPS patterns of **1**: a) survey, and b) F 1s.

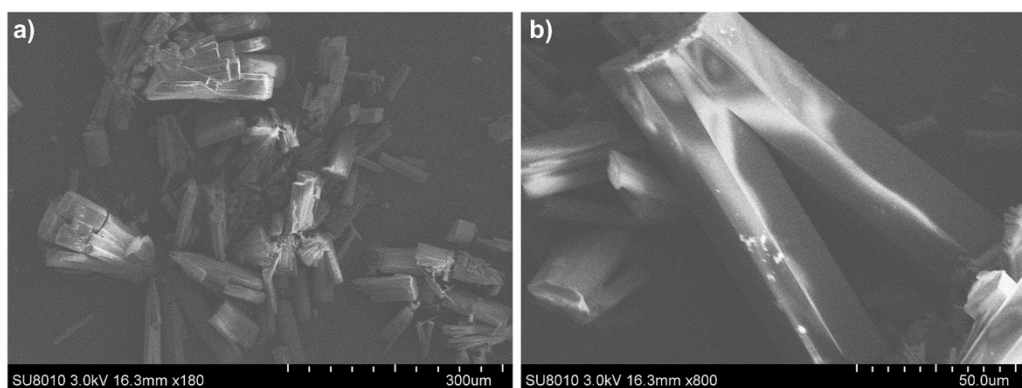


Fig. S3 SEM images of **1**.

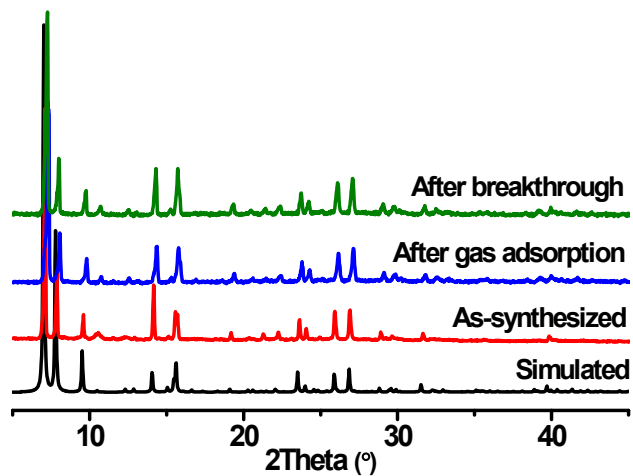


Fig. S4 PXRD of **1** from simulated by single-crystal structure, as-synthesized, desolvated **1a** and samples immersed in the different aqueous solutions.

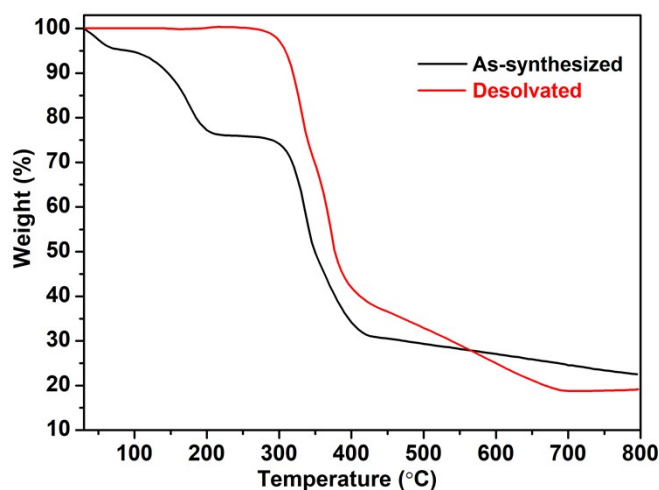


Fig. S5 TGA curves of as-synthesized and desolvated samples of **1**.

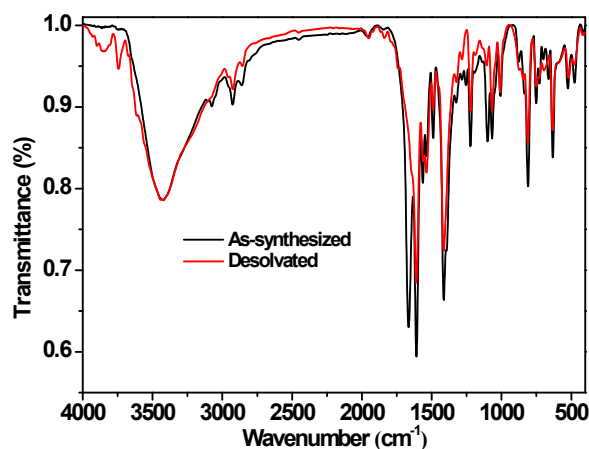


Fig. S6 FTIR spectra of the as-synthesized and desolvated of **1**.

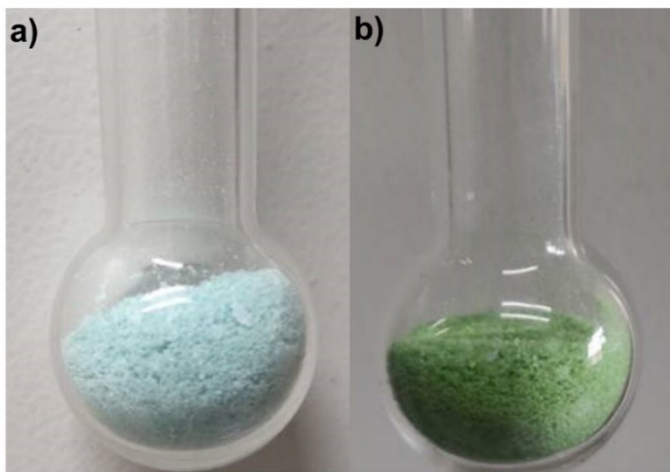


Fig. S7 The color of samples changed a) before and b) after degas.

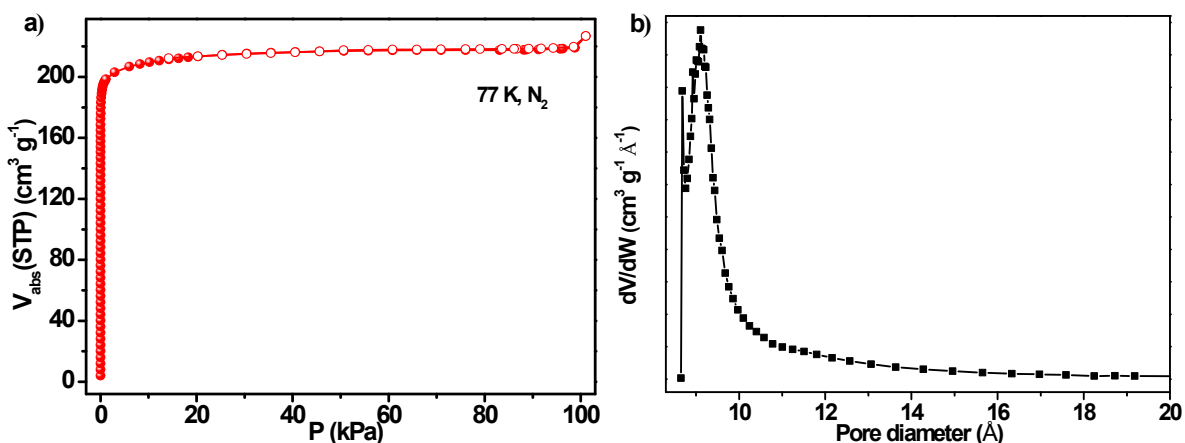


Fig. S8 a) Sorption isotherms of N_2 at 77 K for **1a**, and b) porous distribution plots obtained by the adsorption isotherm of N_2 at 77 K using the Horvath-Kawazoe model.

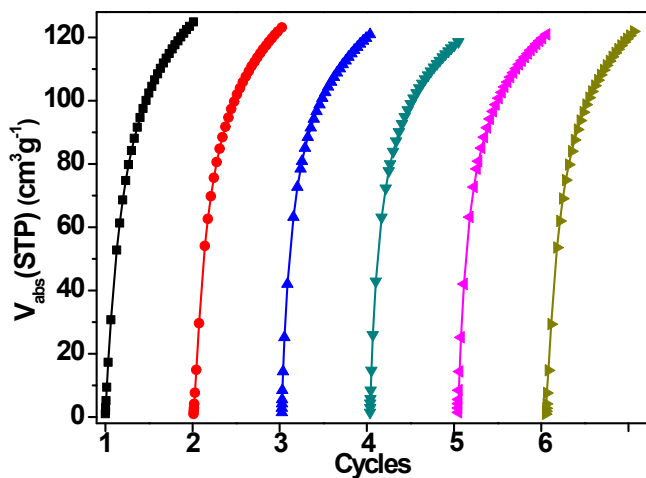


Fig. S9. C_2H_2 uptake of **1a** for 6 cycles at 298 K.

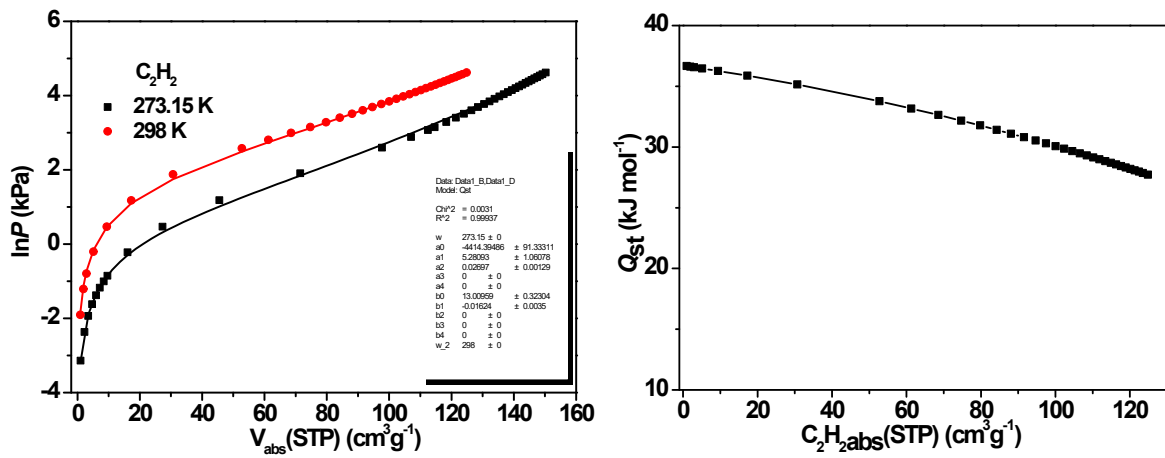


Fig. S10 Fitted C_2H_2 isotherms of **1a** measured at 273.15 and 298 K, and their corresponding isosteric heats of adsorption (Q_{st}).

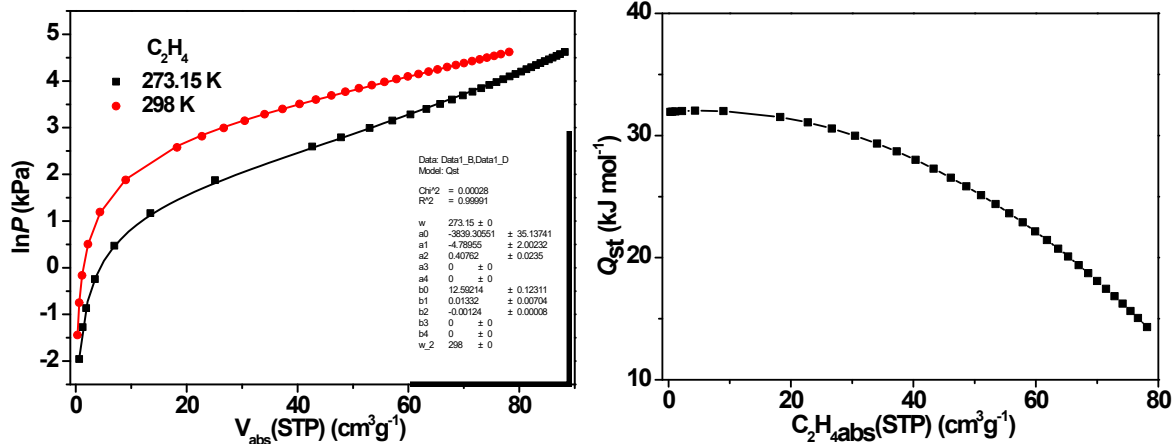


Fig. S11 Fitted C_2H_4 isotherms of **1a** measured at 273.15 and 298 K, and their corresponding isosteric heats of adsorption (Q_{st}).

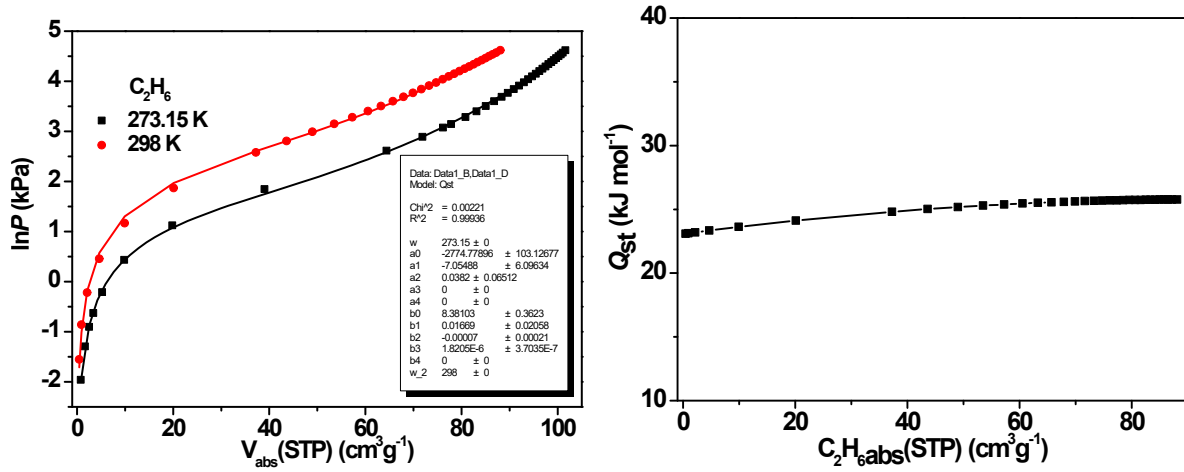


Fig. S12 Fitted C_2H_6 isotherms of **1a** measured at 273.15 and 298 K, and their corresponding isosteric heats of adsorption (Q_{st}).

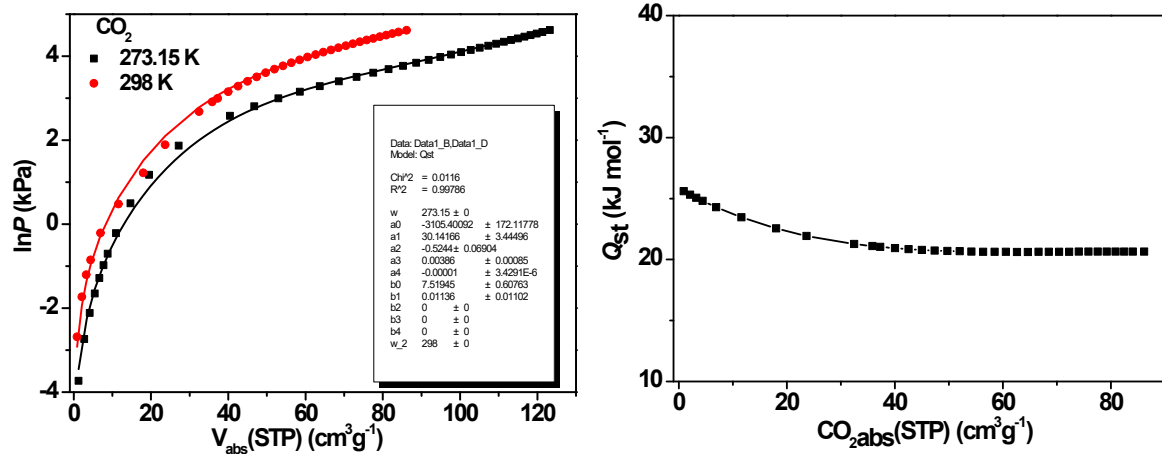


Fig. S13 Fitted CO_2 isotherms of **1a** measured at 273.15 and 298 K, and their corresponding isosteric heats of adsorption (Q_{st}).

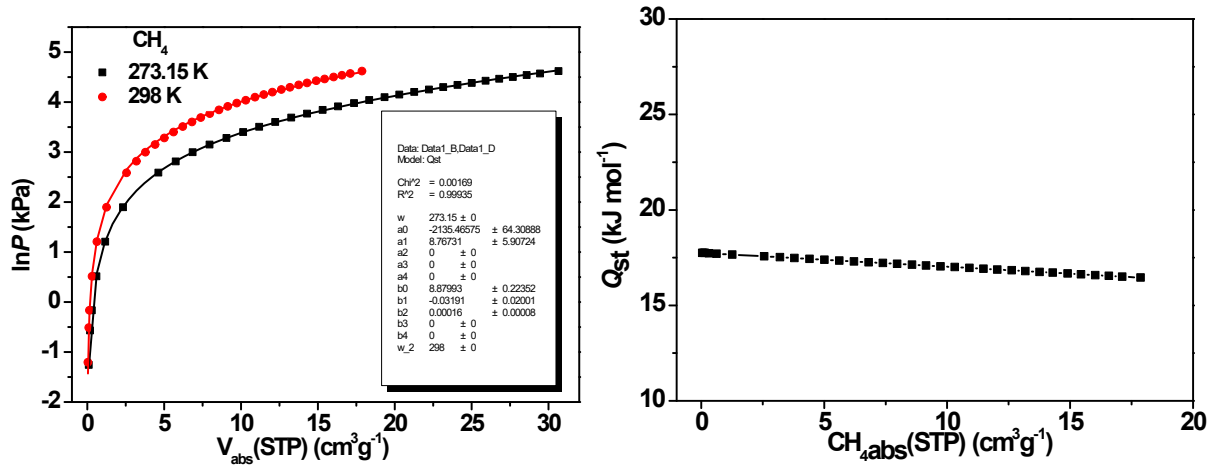


Fig. S14 Fitted CH₄ isotherms of **1a** measured at 273.15 and 298 K, and their corresponding isosteric heats of adsorption (Q_{st}).

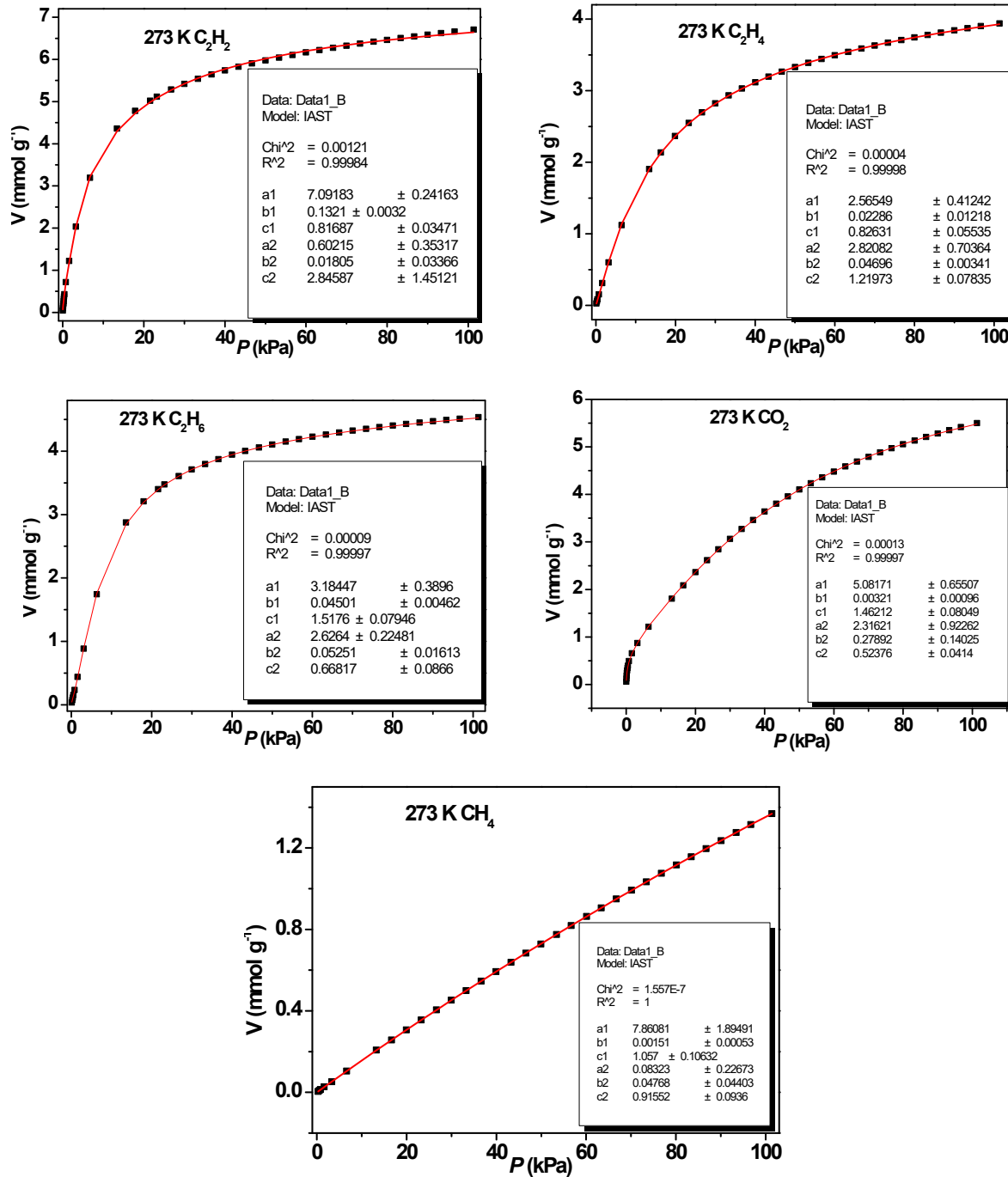


Fig. S15 Adsorption isotherms of **1a** with fitted by dual L-F model at 273 K.

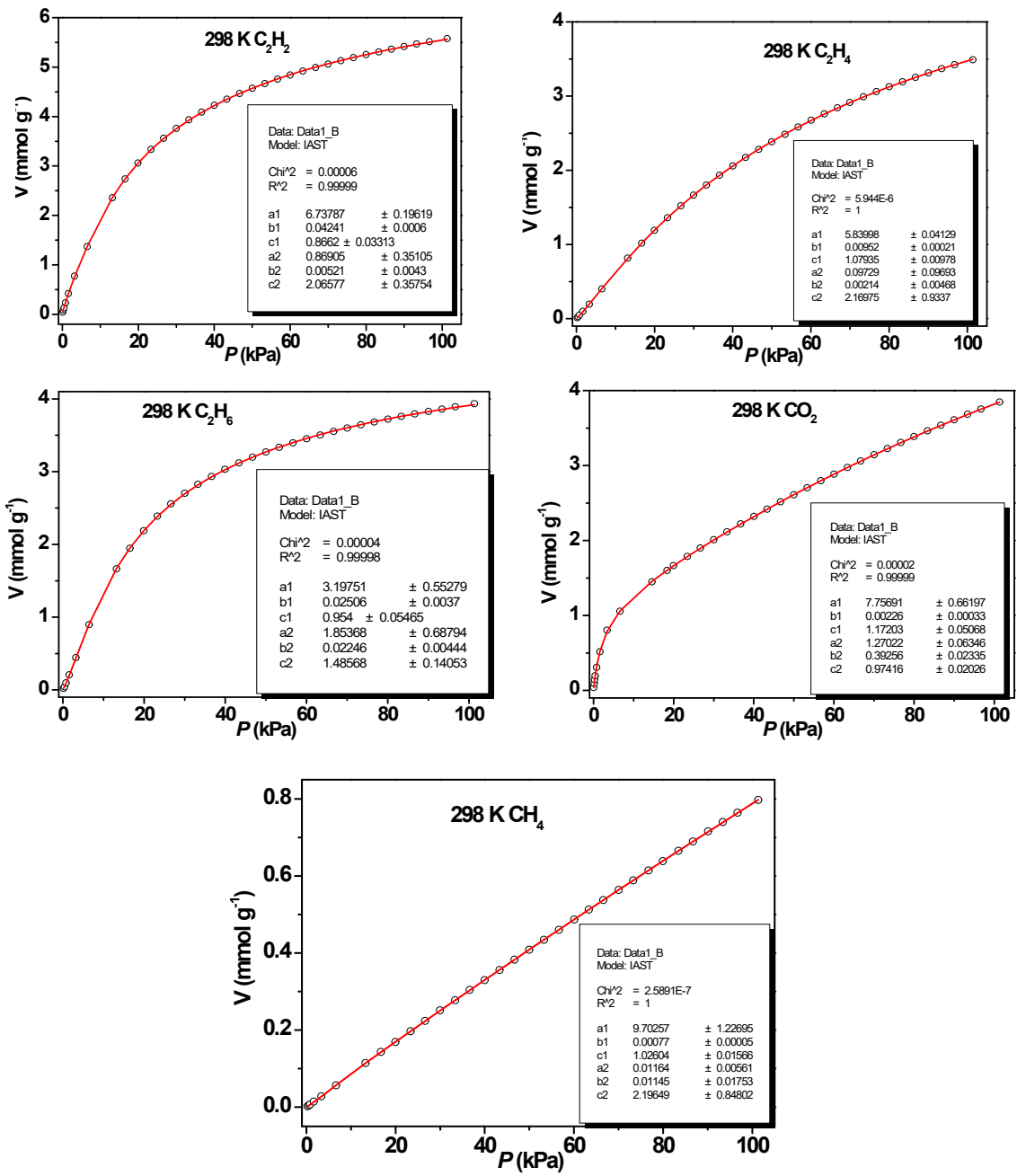


Fig. S16 Adsorption isotherms of **1a** fitted by dual L-F model at 298 K.

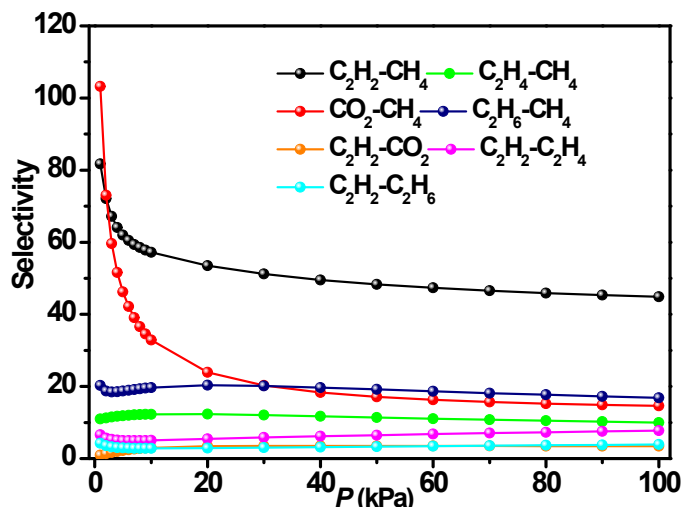


Fig. S17 Adsorption selectivity at 273 K calculated by IAST.

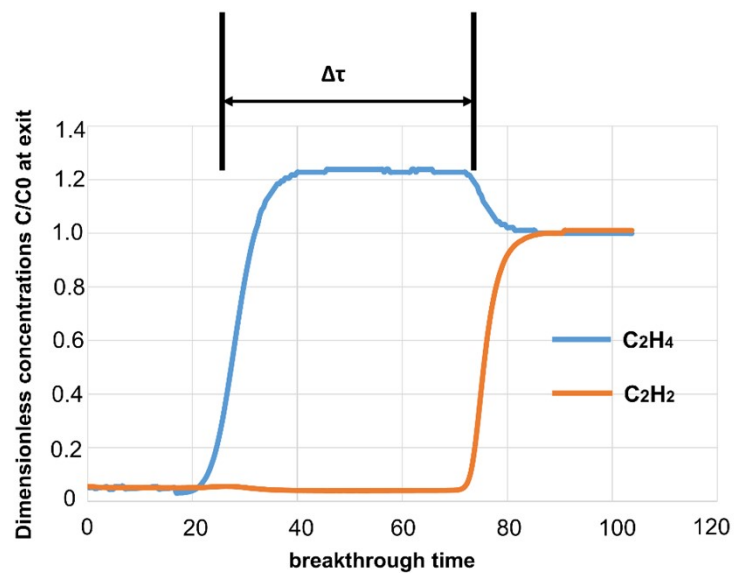


Fig. S18 Breakthrough time intervals ($\Delta\tau$) between C_2H_2 and C_2H_4 ($\text{C}_2\text{H}_2:\text{C}_2\text{H}_4 = 1:1$) for **1a**.

Table S1. Crystallographic data for **1**.

Chemical formula	C ₁₄ H ₁₁ FN ₄ NiO _{1.5}
Formula weight	336.98
T (K)	296(2) K
Crystal system	Orthorhombic
Space group	Pmc ₂ ₁
a (Å)	11.343(3)
b (Å)	12.587(3)
c (Å)	13.755(3)
α (°)	90
β (°)	90
γ (°)	90
V(Å ³)	1963.9(8)
Z	4
D _{calcd.} [g·cm ⁻³]	1.140
μ (mm ⁻¹)	1.001
Reflns collected/unique/R _{int}	10368/3970/0.0771
Goof	0.997
R ₁ ^a , wR ₂ ^b [I > 2σ]	R ₁ = 0.0546, wR ₂ = 0.1148
R ₁ ^a , wR ₂ ^b (all data)	R ₁ = 0.0887, wR ₂ = 0.1312

^aR₁ = Σ(|F_o| - |F_c|) / Σ|F_o|. ^bR₂ = [Σw(F_o² - F_c²)² / Σw(F_o²)²]^{1/2}.

Table S2. Selected bond lengths [Å] and angles [°] for **1**.

Ni(1)-F(2)#1	2.027(11)	F(1)-Ni(1)-N(5)#3	90.9(4)
Ni(1)-F(1)	2.035(10)	O(2)#2-Ni(1)-N(5)#3	89.4(3)
Ni(1)-O(2)#2	2.042(14)	N(5)-Ni(1)-N(5)#3	178.0(8)
Ni(1)-N(5)	2.109(5)	F(2)#1-Ni(1)-N(2)	86.0(5)
Ni(1)-N(5)#3	2.109(5)	F(1)-Ni(1)-N(2)	89.5(5)
Ni(1)-N(2)	2.121(15)	O(2)#2-Ni(1)-N(2)	174.0(7)
Ni(2)-F(2)	1.975(10)	N(5)-Ni(1)-N(2)	90.5(3)
Ni(2)-O(1)	2.011(9)	N(5)#3-Ni(1)-N(2)	90.5(3)
Ni(2)-F(1)#4	2.043(9)	F(2)-Ni(2)-O(1)	171.1(4)
Ni(2)-N(6)#3	2.114(5)	F(2)-Ni(2)-F(1)#4	91.18(19)
Ni(2)-N(6)	2.114(5)	O(1)-Ni(2)-F(1)#4	97.8(4)
Ni(2)-N(3)#5	2.146(16)	F(2)-Ni(2)-N(6)#3	90.9(4)
F(1)-Ni(2)#2	2.043(9)	O(1)-Ni(2)-N(6)#3	89.0(3)
F(2)-Ni(1)#5	2.027(11)	F(1)#4-Ni(2)-N(6)#3	90.6(3)
O(2)-Ni(1)#4	2.042(14)	F(2)-Ni(2)-N(6)	90.9(4)
N(3)-Ni(2)#1	2.146(16)	O(1)-Ni(2)-N(6)	89.0(3)
F(2)#1-Ni(1)-F(1)	175.5(5)	F(1)#4-Ni(2)-N(6)	90.6(3)
F(2)#1-Ni(1)-O(2)#2	88.1(5)	N(6)#3-Ni(2)-N(6)	177.8(4)
F(1)-Ni(1)-O(2)#2	96.4(5)	F(2)-Ni(2)-N(3)#5	81.9(5)
F(2)#1-Ni(1)-N(5)	89.2(4)	O(1)-Ni(2)-N(3)#5	89.1(5)
F(1)-Ni(1)-N(5)	90.9(4)	F(1)#4-Ni(2)-N(3)#5	173.1(5)
O(2)#2-Ni(1)-N(5)	89.4(3)	N(6)#3-Ni(2)-N(3)#5	89.6(4)
F(2)#1-Ni(1)-N(5)#3	89.2(4)	N(6)-Ni(2)-N(3)#5	89.6(4)

^aSymmetry transformations used to generate equivalent atoms: #1 -x+1, -y+1, z-1/2; #2 x, y+1, z; #3 -x+1, y, z; #4 x, y-1, z; #5 -x+1, -y+1, z-1/2.

Table S3. A comparison of high-performance C₂H₂ uptake and Q_{st} for MOFs at 298 K.

MOFs	D_1	G	V	D_2	initial Q_{st}	Ref.
	(g cm ⁻³)	(cm ³ g ⁻¹)	(cm ³ cm ⁻³)	(g cm ⁻³)	(kJ mol ⁻¹)	
1a	1.140	124.8	142	0.17	36.7	This work
FJI-H8	0.876	224	196	0.23	32	1
[Co ₂ (DHTP)]	1.169	197	230	0.27	50.1	2
HKUST-1	0.879	201	177	0.21	30.4	3
SIFSIX-Cu-TPA	0.995	185	184	0.21	39.1	4
FJU-90	0.816	183	149	0.17	25.2	5
Cu-CPAH	1.317	132	174	0.20	35.4	6
SNNU-27-Ni	0.763	159.0	121	0.14	23.1	7
SNNU-26-Co	0.832	155.6	129	0.15	26.6	7
ZJNU-69	0.930	171.7	159	0.18	31.2	8
SNNU-61	1.163	142.1	165	0.19	38.2	9
SNNU-65-Cu-Ca	0.682	141.6	96	0.11	31.7	10
NCU-100	1.535	102	156	0.18	60.5	11
PCN-33	1.327	122	162	0.19	27.3	12
[Co(btzip)(H ₂ btzip)]	1.184	121	143	0.17	37.3	13
[Co ₂ (L) ₂ (BDC-Br)(H ₂ O)]	1.401	121.4	170	0.19	/	14
Tm ₂ (OH-bdc) ₂ (μ ₃ -OH) ₂	1.191	118	140	0.16	17.8	15
MOF-505	0.927	148	137	0.16	24.7	3
NPU-1	0.957	114.2	109	0.13	27.88	16
NPU-2	0.830	90.2	86	0.1	20.98	16
NPU-3	0.732	57.7	42	0.05	19.93	16
ZJNU-34(NH ₂)	0.7064	194	137	0.16	34.2	17
ZJNU-37(F)	0.7013	171.5	120.3	0.14	33.6	17
[Cu _{0.5} (tztp) _{0.5}]	1.205	112	135	0.16	38.3	18
MECS-5a	1.369	86	118	0.14	26.09	19
ZJU-74a	1.353	86	115	0.13	45	20

[Ni(dpip)]	0.807	83.6	67	0.08	41.7	21
SNNU-45	0.844	134	113	0.13	39.9	22
FJU-6-TATB	0.928	110	102	0.12	29	23
UTSA-74a	1.34	145.0	194	0.22	31	24
Sc-EBTC	0.872	88	77	0.09	22.6	25
NbU-1	1.225	60	74	0.09	38.3	26
SNNU-28-Co	0.742	58.2	43	0.05	31.5	7
JLU-MOF66	1.348	55	74	0.09	35.6	27
BSF-1	1.046	52.6	55	0.06	31	28
ZIF-8	0.924	25	23	0.03	13.3	3
MOF-5	0.590	26	15	0.02	16.1	3

Table S4. Gas adsorption results of **1a**.

1a	S _{BET} (m ² /g)	Pore sizes	Adsorption uptake (cm cm ⁻³)						Q _{st} at Zero Coverage (kJ mol ⁻¹)			
			C ₂ H ₂	C ₂ H ₄	C ₂ H ₆	CH ₄	CO ₂	C ₂ H ₂	C ₂ H ₄	C ₂ H ₆	CH ₄	CO ₂
			700	7 Å								
273 K			171	101	115	35	140					
298 K			142	89	100	20	98	36.7	31.9	23.1	17.8	25.6

Table S5. Summary of C₂H₂ and CO₂ uptakes and C₂H₂-CO₂ and CO₂-CH₄ selectivity for different MOFs at 298 K under 100 kPa.

MOFs	C ₂ H ₂ /CO ₂ Uptakes (mmol g ⁻¹)	C ₂ H ₂ -CO ₂ selectivity	CO ₂ -CH ₄ selectivity	Ref.
1a	5.57/3.84	2.2/3.4 ^c	15.2/14.6 ^c	This work
[Cu _{0.5} (tztp) _{0.5}]	5.0/3.40	2.7	6.5	18
FJU-6-TATB	4.91 ^b / 2.58 ^b	3.1 ^b	NA	23
Zn-MOF-74	5.52 / 5.38	2	NA	24
BSF-1	2.35/1.77	3.3	7.5	28
[Cd(dtztp) _{0.5} (HCOO)]	3.57/2.87	2	14.8	29
PCM-48	1.14/NA	4.3 ^b	6.1	30
MIL-53(Al)	NA/1.3 ^a	NA	7	31
[Zn ₁₂ (tdc) ₆ (EgO ₂) ₆ (dabco) ₃]	1.95/1.80	3.3/4.4 ^c	2.9/3.3 ^c	32
[Zn ₁₂ (tdc) ₆ (PrO ₂) ₆ (dabco) ₃]	2.33/2.03	1.1/1.1 ^c	3.8/4.5 ^c	32
[Zn ₁₂ (tdc) ₆ (BuO ₂) ₆ (dabco) ₃]	2.22/1.76	1.4/2.0 ^c	3.1/3.9 ^c	32
NTU-56	1.59 ^c / 1.14 ^c	1/2.3 ^c	NA	33
SNNU- 5-In	6.9 ^c / 3.24 ^c	2.6 ^c	3.9 ^c	34
SNNU-13	3.17/1.94	3.5/3.1 ^c	7.6/21.6 ^c	35
NbU-10	3.51 ^c / 2.63 ^c	6.5/6.6 ^c	NA	36

*a: measured at 303 K; b: measured at 296 K; c: measured at 273 K; NA = not available

Table S6. Summary of C₂H_n/CH₄ selectivity for different MOFs at 273 and 298 K under 100 kPa.

MOFs	Temperatur e (K)	IAST selectivity			Ref.
		C ₂ H ₂ -CH ₄	C ₂ H ₄ -CH ₄	C ₂ H ₆ -CH ₄	
1a	273	44.8	10.0	16.9	This work
	298	25.9	7.5	15.1	
SNNU-5-In	273	10.0	7.4	NA	34
SNNU-13	273	114.9	40.2	NA	35
	298	48.5	20	NA	
HCP-B	273	14.1	10.6	14.1	37
	298	9.6	6.0	8.1	
NOTT-101	273	36.9	30.0	11.1	38
	298	22.2	18.6	14.1	
Cu _{0.5} (tztp) _{0.5}	298	23.0	11.3	16.1	18
ZnSDB	273	18.6	17.6	20.6	39
	298	16.9	15.9	23.2	
Sc-ABTC	273	28.4	19.9	NA	25
	298	14.7	11.7	NA	
ZJNU-63	298	13.1	7	10.6	40
LIFM-WZ-3	273	NA	17.3	9.8	41
	298	NA	26.8	10.7	
SNNU-64	273	45.7	42.7	NA	42
	298	35.8	24.3	NA	
[Zn ₁₂ (tdc) ₆ (PrO ₂) ₆ (dabco) ₃]	273	3.6	3.9	5.6	32
	298	3.0	5.5	4.7	

NA = not available.

Table S7. Summary of C₂H₂-C₂H₄ and C₂H₂-C₂H₆ selectivity for different materials at 273 and 298 K under 100 kPa.

Materials	Gas selectivity	IAST selectivity		Ref.
		273 K	298 K	
1a	C ₂ H ₂ -C ₂ H ₄	7.7	4.0	This work
	C ₂ H ₂ -C ₂ H ₆	3.9	2.1	
Na-ZM	C ₂ H ₂ -C ₂ H ₆	4.2	NA	43
	C ₂ H ₂ -C ₂ H ₄	1	NA	
YAU-7	C ₂ H ₂ -C ₂ H ₄	1.30	1.5	44
MgMOF-74	C ₂ H ₂ -C ₂ H ₄	NA	2.18	19
CoMOF-74	C ₂ H ₂ -C ₂ H ₄	NA	1.70	
NOTT-300	C ₂ H ₂ -C ₂ H ₄	NA	2.17	
UTSA-60a	C ₂ H ₂ -C ₂ H ₄	NA	~5.5	
UTSA-67a	C ₂ H ₂ -C ₂ H ₄	NA	5	45
NbU-1	C ₂ H ₂ -C ₂ H ₄	12.1	5.9	26
Zn ₂ (Atz) ₂ O _x	C ₂ H ₂ -C ₂ H ₄	NA	1.74	46
HUST-5	C ₂ H ₂ -C ₂ H ₄	1.8	NA	47
SNNU-95	C ₂ H ₂ -C ₂ H ₄	NA	1.7	48
BSF-1	C ₂ H ₂ -C ₂ H ₄	NA	2.3	28
PAF-110	C ₂ H ₂ -C ₂ H ₄	NA	3.9	49
CTF-PO71	C ₂ H ₂ -C ₂ H ₄	NA	1.8	50
M'MOF-3a	C ₂ H ₂ -C ₂ H ₄	NA	1.6 ^a	51
Fe ₂ (dobdc)	C ₂ H ₂ -C ₂ H ₄	NA	1.87	52

*a: measured at 296 K; NA = not available

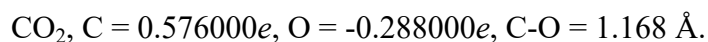
Table S8. Comparison of stability for some top-performing C₂H₂ separation MOFs.

MOFs	Water	pH = 2	pH = 12	Thermal stability	Ref.
1a	✓	✓	✓	290 °C	This work
UiO-66	✓	✓	✓	500 °C	53
ZIF-8	✓	✓	✓	450°C	54
bio-MOF-1	✓	a	a	180 °C	55
FeNi-M' MOF	✓	a	a	200 °C	56
JCM-1	✓	✗	✗	300 °C	57
UTSA-300	✗	✗	✗	200 °C	58
ATC-Cu	✓	a	a	270 °C	59
HOF-3	✗	✗	✗	350 °C	60
NKMOF-1-Ni	✓	✓	✓	240 °C	61
MUF-16	✓	a	a	330 °C	62
Tm ₂ (OH-bdc) ₂ (μ ₃ -OH) ₂ (H ₂ O) ₂	✓	a	a	400 °C	15
PCP-NH ₂ -ipa	✓	a	a	280 °C	63
Azole-Th-1	✓	✓	✓	200 °C	64
UPC-612	✓	✓	✓	300 °C	65
Ca(squareate)	✓	a	a	400 °C	66
UTSA-74	✗	✗	✗	200 °C	24
SNNU-27-Fe	✓	✓	✓	320 °C	7
ZJU-74	✓	✓	✓	300 °C	20
JNU-1	✓	✗	✓	450 °C	67

^a The stability in the corresponding conditions was not reported in the literatures.

Molecular Simulation

Grand canonical Monte Carlo (GCMC) simulations were performed for the gas adsorption in the framework by the Sorption module of Material Studio (Accelrys. Materials Studio Getting Started, release 5.0). The framework was considered to be rigid, and the optimized gas and epoxide molecules were used. The atom charges and bond lengths for the gas molecules are as follows:



C_2H_2 , C = -0.238847 e, H = 0.238847 e, C-C = 1.198 Å, C-H = 1.065 Å.

C_2H_4 , C = -0.295071 e, H = 0.147536 e, C-C = 1.334 Å, C-H = 1.090 Å.

C_2H_6 , C = -0.458757 e, H = 0.152919 e, C-C = 1.528 Å, C-H = 1.099 Å.

The partial atom charges of the framework were derived from QE_q method and QE_q neutral 1.0 parameter (Table S9). One unit cell was used during the simulations. The interaction energies between the gas molecules and framework were computed through the Coulomb and Lennard-Jones 6-12 (LJ) potentials. All parameters for the atoms were modeled with the universal force field (UFF) embedded in the MS modeling package. A cutoff distance of 12.5 Å was used for LJ interactions, and the Coulombic interactions were calculated by using Ewald summation. For each run, the 5×10^6 maximum loading steps, 5×10^6 production steps were employed.

Table S9. The atomic partial charges (e) in the framework.

Ni1	1.13529	N6	-0.251918	C7	-0.155383	C16	0.0346167	H12	0.0930945
Ni2	1.13395	O1	-0.550478	C8	0.518427	C17	-0.158774	H13	0.133209
F1	-0.564701	O2	-0.534282	C9	0.0158995	C18	0.00154532	H14	0.135115
F2	-0.565625	C1	0.274925	C10	-0.155723	H3	0.132791	H15	0.0912609
N1	-0.281485	C2	0.0326761	C11	0.0351438	H4	0.146805	H17	0.0976686
N2	-0.0888034	C3	-0.153385	C12	-0.153645	H6	0.142385	H18	0.133851
N3	-0.0752667	C4	-0.162513	C13	0.0259178	H7	0.129243		
N4	-0.301747	C5	0.0139411	C14	0.0534890	H9	0.134649		
N5	-0.255173	C6	-0.158681	C15	-0.139020	H10	0.0947561		

References:

- 1) J. Pang, F. Jiang, M. Wu, C. Liu, K. Su, W. Lu, D. Yuan and M. Hong, *Nat. Commun.*, 2015, **6**, 7575.
- 2) S.-C. Xiang, W. Zhou, Z.-J. Zhang, M. A. Green, Y. Liu and B. Chen, *Angew. Chem., Int. Ed.*, 2010, **49**, 4615.
- 3) S. Xiang, W. Zhou, J. M. Gallegos, Y. Liu and B. Chen, *J. Am. Chem. Soc.*, 2009, **131**, 12415.
- 4) H. Li, C. Liu, C. Chen, Z. Di, D. Yuan, J. Pang, W. Wei, M. Wu and M. Hong, *Angew. Chem. Int. Ed.*, 2021, **60**, 7547-7552.

- 5) Y. Ye, Z. Ma, R.-B. Lin, R. Krishna, W. Zhou, Q. Lin, Z. Zhang, S. Xiang and B. Chen, *J. Am. Chem. Soc.*, 2019, **141**, 4130-4136.
- 6) L. Meng, L. Yang, C. Chen, X. Dong, S. Ren, G. Li, Y. Li, Y. Han, Z. Shi and S. Feng, *ACS Appl. Mater. Interfaces*, 2020, **12**, 5999-6006.
- 7) Y.-Y. Xue, X.-Y. Bai, J. Zhang, Y. Wang, S.-N. Li, Y.-C. Jiang, M.-C. Hu and Q.-G. Zhai, *Angew. Chem. Int. Ed.*, 2021, **60**, 10122-10128.
- 8) F. Chen, Y. Wang, D. Bai, M. He, X. Gao and Y. He, *J. Mater. Chem. A*, 2018, **6**, 3471-3478.
- 9) J.-W. Zhang, M.-C. Hu, S.-N. Li, Y.-C. Jiang and Q.-G. Zhai, *Chem. Eur. J.*, 2017, **23**, 6693-6700.
- 10) J.-W. Zhang, M.-C. Hu, S.-N. Li, Y.-C. Jiang, P. Qu and Q.-G. Zhai, *Chem. Commun.*, 2018, **54**, 2012-2015.
- 11) J. Wang, Y. Zhang, P. Zhang, J. Hu, R.-B. Lin, Q. Deng, Z. Zeng, H. Xing, S. Deng and B. Chen, *J. Am. Chem. Soc.*, 2020, **142**, 9744-9751.
- 12) J. Duan, W. Jin and R. Krishna, *Inorg. Chem.*, 2015, **54**, 4279-4284.
- 13) Y.-Z. Li, G.-D. Wang, W.-J. Shi, L. Hou, Y.-Y. Wang and Z. Zhu, *ACS Appl. Mater. Interfaces*, 2020, **12**, 41785-41793.
- 14) P.-P. Cui, X.-D. Zhang, Y.-S. Kang, Y. Zhao and W.-Y. Sun, *Inorg. Chem.*, 2021, **60**, 2563-2572.
- 15) D. Ma, Z. Li, J. Zhu, Y. Zhou, L. Chen, X. Mai, M. Liufu, Y. Wu and Y. Li, *J. Mater. Chem. A*, 2020, **8**, 11933-11937.
- 16) B. Zhu, J.-W. Cao, S. Mukherjee, T. Pham, T. Zhang, T. Wang, X. Jiang, K. A. Forrest, M. J. Zaworotko and K.-J. Chen, *J. Am. Chem. Soc.*, 2021, **143**, 1485-1492.
- 17) F. Chen, D. Bai, X. Wang and Y. He, *Inorg. Chem. Front.*, 2017, **4**, 960-967.
- 18) X.-Y. Li, Y.-Z. Li, L.-N. Ma, L. Hou, C.-Z. He, Y.-Y. Wang and Z. Zhu, *J. Mater. Chem. A*, 2020, **8**, 5227.
- 19) X.-J. Hong, Q. Wei, Y.-P. Cai, B. Wu, H.-X. Feng, Y. Yu and R.-F. Dong, *ACS Appl. Mater. Interfaces*, 2017, **9**, 29374-29379.
- 20) J. Pei, K. Shao, J.-X. Wang, H.-M. Wen, Y. Yang, Y. Cui, R. Krishna, B. Li and G. Qian,

- Adv. Mater.*, 2020, **1**, 1908275.
- 21) Y.-Z. Li, G.-D. Wang, L.-N. Ma, L. Hou, Y.-Y. Wang and Z. Zhu, *ACS Appl. Mater. Interfaces*, 2021, **13**, 4102-4109.
- 22) Y.-P. Li, Y. Wang, Y.-Y. Xue, H.-P. Li, Q.-G. Zhai, S.-N. Li, Y.-C. Jiang, M.-C. Hu and X. Bu, *Angew. Chem. Int. Ed.*, 2019, **58**, 13590-13595.
- 23) L. Liu, Z. Yao, Y. Ye, Y. Yang, Q. Lin, Z. Zhang, M. O'Keeffe and S. Xiang, *J. Am. Chem. Soc.*, 2020, **142**, 9258-9266.
- 24) F. Luo, C. Yan, L. Dang, R. Krishna, W. Zhou, H. Wu, X. Dong, Y. Han and T.-L. Hu, *J. Am. Chem. Soc.*, 2016, **138**, 5678-5684.
- 25) J.-W. Zhang, P. Qu, M.-C. Hu, S.-N. Li, Y.-C. Jiang and Q.-G. Zhai, *Inorg. Chem.*, 2019, **58**, 16792-16799.
- 26) J. Li, L. Jiang, S. Chen, A. Kirchon, B. Li, Y. Li and H.-C. Zhou, *J. Am. Chem. Soc.*, 2019, **141**, 3807-3811.
- 27) L. Kan, G. Li and Y. Liu, *ACS Appl. Mater. Interfaces*, 2020, **12**, 18642-18649.
- 28) Y. Zhang, L. Yang, L. Wang, S. Duttwyler and H. Xing, *Angew. Chem., Int. Ed.*, 2019, **58**, 8145-8150.
- 29) G.-D. Wang, Y.-Z. Li, W.-J. Shi, L. Hou, Z. Zhu and Y.-Y. Wang, *Inorg. Chem. Front.*, 2020, **7**, 1957-1964.
- 30) J. E. Reynolds, III, K. M. Walsh, B. Li, P. Kunal, B. Chen and S. M. Humphrey, *Chem. Commun.*, 2018, **54**, 9937-9940.
- 31) V. Finsy, L. Ma, L. Alaerts, D. E. D. Vos, G. V. Baron and J. F. M. Denayer, *Microporous Mesoporous Mater.*, 2009, **120**, 221.
- 32) A. A. Lysova, D. G. Samsonenko, P. V. Dorovatovskii, V. A. Lazarenko, V. N. Khrustalev, K. A. Kovalenko, D. N. Dybtsev and V. P. Fedin, *J. Am. Chem. Soc.*, 2019, **141**, 17260-17269.
- 33) H. Wang, N. Behera, S. Wang, Q. Dong, Z. Wang, B. Zheng, D. Wang and J. Duan, *Inorg. Chem. Front.*, 2020, **7**, 3195-3203.
- 34) J.-W. Zhang, W.-J. Ji, M.-C. Hu, S.-N. Li, Y.-C. Jiang, X.-M. Zhang, P. Qu and Q.-G. Zhai, *Inorg. Chem. Front.*, 2019, **6**, 813-819.
- 35) H.-P. Li, Z.-D. Dou, Y. Wang, Y. Y. Xue, Y. P. Li, M.-C. Hu, S.-N. Li, Y.-C. Jiang and

- Q.-G. Zhai, *Inorg. Chem.*, 2020, **59**, 16725-16736.
- 36) J. Zhao, Q. Li, X. Zhu, J. Li and D. Wu, *Inorg. Chem.*, 2020, **59**, 14424-14431.
- 37) J. Chen, L. Jiang, C. Li, W. Fu, Q. Xia, Y. Wang and Y. Huang, *Polym. Eng. Sci.*, 2021, **61**, 662-668.
- 38) J. Li, S. Chen, L. Jiang, D. Wu and Y. Li, *Inorg. Chem.*, 2019, **58**, 5410-5413.
- 39) F.-S. Tang, R.-B. Lin, R.-G. Lin, J. C.-G. Zhao and B. Chen, *J. Solid State Chem.*, 2018, **258**, 346-350.
- 40) D. Bai, Y. Wang, M. He, X. Gao and Y. He, *Inorg. Chem. Front.*, 2018, **5**, 2227-2237.
- 41) Z. Wang, J.-H. Zhang, J.-J. Jiang, H.-P. Wang, Z.-W. Wei, X. Zhu, M. Pan and C.-Y. Su, *J. Mater. Chem. A*, 2018, **6**, 17698-17705.
- 42) J.-W. Zhang, P. Qu, M.-C. Hu, S.-N. Li, Y.-C. Jiang and Q.-G. Zhai, *Cryst. Growth Des.*, 2020, **20**, 5657-5663
- 43) J. Wang, Q. Zhu, Z. Zhang, M. Sadakane, Y. Li and W. Ueda, *Angew. Chem. Int. Ed.*, 2021, **60**, 18328-18334.
- 44) S.-Y. Li, F.-F. Zhang, X. Wang, M.-H. He, Z. Ding, M. Chen, X.-Y. Hou, X.-L. Chen, L. Tang, E.-L. Yue, J.-J. Wang and F. Fu, *J. Solid State Chem.*, 2021, **294**, 121896.
- 45) H.-M. Wen, B. Li, H. Wang, R. Krishnab and B. Chen, *Chem. Commun.*, 2016, **52**, 1166-1169
- 46) P.-D. Zhang, X.-Q. Wu, T. He, L.-H. Xie, Q. Chen and J.-R. Li, *Chem. Commun.*, 2020, **56**, 5520-5523.
- 47) F. Yu, B.-Q. Hu, X.-N. Wang, Y.-M. Zhao, J.-L. Li, B. Li and H. -C. Zhou, *J. Mater. Chem. A*, 2020, **8**, 2083-2089.
- 48) H. Li, S. Li, X. Hou, Y. Jiang, M. Hua and Q.-G. Zhai, *Dalton Trans.*, 2018, **47**, 9310-9316.
- 49) L. Jiang, Y. Tian, T. Sun, Y. Zhu, H. Ren, X. Zou, Y. Ma, K. R. Meihaus, J. R. Long and G. Zhu, *J. Am. Chem. Soc.*, 2018, **140**, 15724-15730.
- 50) Y. Lu, J. He, Y. Chen, H. Wang, Y. Zhao, Y. Han and Y. Ding, *Macromol. Rapid Commun.*, 2018, **39**, 1700468.
- 51) S.-C. Xiang, Z. Zhang, C.-G. Zhao, K. Hong, X. Zhao, D.-R. Ding, M.-H. Xie, C.-D. Wu, M. C. Das, R. Gill, K. M. Thomas and B. Chen, *Nat. Commun.*, 2011, **2**, 204

- 52) E. D. Bloch, W. L. Queen, R. Krishna, J. M. Zadrozny, C. M. Brown and J. R. Long, *Science*, 2012, **335**, 1606-1610.
- 53) M. J. Katz, Z. J. Brown, Y. J. Colón, P. W. Siu, K. A. Scheidt, R. Q. Snurr, J. T. Hupp and O. K. Farha, *Chem. Commun.*, 2013, **49**, 9449-9451.
- 54) Y. Pan, Y. Liu, G. Zeng, L. Zhao and Z. Lai, *Chem. Commun.*, 2011, **47**, 2071-2073.
- 55) J. An, S. J. Geib and N. L. Rosi, *J. Am. Chem. Soc.*, 2009, **131**, 8376-8377.
- 56) J. Gao, X. Qian, R.-B. Lin, R. Krishna, H. Wu, W. Zhou and B. Chen, *Angew. Chem. Int. Ed.*, 2020, **59**, 4396-4400.
- 57) J. Lee, C. Y. Chuah, J. Kim, Y. Kim, N. Ko, Y. Seo, K. Kim, T. H. Bae and E. Lee, *Angew. Chem., Int. Ed.*, 2018, **57**, 7869-7873.
- 58) R.-B. Lin, L. Li, H. Wu, H. Arman, B. Li, R.-G. Lin, W. Zhou and B. Chen, *J. Am. Chem. Soc.*, 2017, **139**, 8022-8028.
- 59) Z. Niu, X. Cui, T. Pham, G. Verma, P. C. Lan, C. Shan, H. Xing, K. A. Forrest, S. Suepaul, B. Space, A. Nafady, A. M. Al-Enizi and S. Ma, *Angew. Chem. Int. Ed.*, 2021, **60**, 5283-5288.
- 60) P. Li, Y. He, Y. Zhao, L. Weng, H. Wang, R. Krishna, H. Wu, W. Zhou, M. O'Keeffe, Y. Han and B. Chen, *Angew. Chem. Int. Ed.*, **2015**, *54*, 574-577.
- 61) Y.-L. Peng, T. Pham, P. Li, T. Wang, Y. Chen, K.-J. Chen, K. A. Forrest, B. Space, P. Cheng, M. J. Zaworotko and Z. Zhang, *Angew. Chem. Int. Ed.*, 2018, **57**, 10971-10975.
- 62) O. T. Qazvini, R. Babarao and S. G. Telfer, *Nat. Commun.*, 2021, **12**, 197.
- 63) Y. Gu, J.-J. Zheng, K. Otake, M. Shivanna, S. Sakaki, H. Yoshino, M. Ohba, S. Kawaguchi, Y. Wang, F. Li and S. Kitagawa, *Angew. Chem. Int. Ed.*, 2021, **60**, 11688-11694.
- 64) Z. Xu, X. Xiong, J. Xiong, R. Krishna, L. Li, Y. Fan, F. Luo and B. Chen, *Nat. Commun.*, 2020, **11**, 3163.
- 65) Y. Wang, C. Hao, W. Fan, M. Fu, X. Wang, Z. Wang, L. Zhu, Y. Li, X. Lu, F. Dai, Z. Kang, R. Wang, W. Guo, S. Hu and D. Sun, *Angew. Chem. Int. Ed.*, 2021, **60**, 11350-11358.
- 66) L. Li, L. Guo, S. Pu, J. Wang, Q. Yang, Z. Zhang, Y. Yang, Q. Ren, S. Alnemrat and Z.

- Bao, *Chem. Eng. J.*, 2019, **358**, 446-455.
- 67) H. Zeng, M. Xie, Y.-L. Huang, Y. Zhao, X.-J. Xie, J.-P. Bai, M.-Y. Wan, R. Krishna, W. Lu and D. Li, *Angew. Chem., Int. Ed.*, 2019, **58**, 8515-8519.